Biochimica et Biophysica Acta 1838 (2014) 2788–2797

Contents lists available at ScienceDirect

Biochimica et Biophysica Acta

journal homepage: www.elsevier.com/locate/bbamem

Three dimensional (temperature–tension–composition) phase map of mixed DOPC–DPPC vesicles: Two solid phases and a fluid phase coexist on three intersecting planes

Dong Chen [a], Maria M. Santore [b,*]

[a] Department of Physics, University of Massachusetts, Amherst, MA 01003, USA
[b] Department of Polymer Science and Engineering, University of Massachusetts, Amherst, MA 01003, USA

ARTICLE INFO

Article history:
Received 30 April 2014
Received in revised form 23 June 2014
Accepted 16 July 2014
Available online 23 July 2014

Keywords:
Phospholipid phase separation
Phospholipid phase diagram
Membrane tension
Solid domain shape
Coexistence
Equilibrium

ABSTRACT

Mapping the phase behavior of multicomponent phospholipid membranes has been an ongoing pursuit, motivated by interest in both fundamental physics and cell function. Prior investigations addressed temperature-composition space and the features of the associated domains. The current study additionally considers membrane tension, analogous to pressure in bulk materials. Focusing on model mixed 1,2-dioleoyl-sn-glycero-3-phosphocholine and 1,2-dipalmitoyl-sn-glycero-3-phosphocholine (DOPC and DPPC respectively) membranes, we examine the thermodynamic impact of tension on fluid-solid coexistence and the nature of phase-separated domains. Reported here is the 3 dimensional composition-temperature-tension phase map containing three intersecting curved surfaces. Depending on the system's position in this 3D space, giant unilamellar vesicles containing DOPC and DPPC may exhibit, in addition to a 2-component fluid Lα phase, two different types of solid DPPC-rich domains: tracer-excluding hexagonal patches or tracer-selective stripes. The fluid phase occurs at high temperatures. At cool temperatures striped solid DPPC-rich domains coexist with the fluid at elevated tensions. These stripes occur independent of tension, at the coolest temperatures. At low tensions and intermediate temperatures, patchy solid DPPC-rich domains coexist with the Lα fluid and may persist, if kinetically trapped, at lower temperatures. We associate the striped DPPC domains with a tilt-gel (Lβ') morphology and the hexagonal DPPC patches with a dense corrugated ripple phase (Pβ'). These assignments, based on the reported areal densities of the corrugated and tilt solids, enabled first principles estimates of the coexistence boundaries that match the experiments well, including the tension sensitivity of coexistence curves and triple-point-like features for fixed composition.

1. Introduction

The possibility that phospholipid rafts cluster functionality within a cell membrane to regulate signaling and trafficking has fueled interest in the phase behavior of phospholipid membranes [1,2]. A fascinating prospect for signaling mechanisms involving membrane domains is the potential for changes in local membrane tension to drive membrane restructuring, so that a cell's surface physically transduces mechanical stimuli. Such a possibility raises fundamental questions about the influence of tension on the phase behavior of multicomponent membranes. While the interplay between tension, curvature, and domain size and shape has come to the forefront [3–7], the more global influence of tension on the thermodynamic equilibrium of multicomponent membranes has not been broadly explored. The paucity of studies of the thermodynamic impact of tension registers a stark contrast with the large body of literature on the temperature–composition dependence of fluid–fluid [8–13] and fluid–solid [14–20] transitions in multicomponent membranes.

A few recent investigations examined the impact of tension on the miscibility within multicomponent fluid membranes. Of these, Ayuyan and Cohen report that tension, resulting from osmotic swelling of biological vesicles, increases the appearance of raft domains [21]. They point out, however, that these and similar observations by others [3] might have resulted from the impact of membrane tension on the line tension of the domains, driving fluid domain coalescence (increasing visibility) rather than a true shifting from the miscible to two-phase region of thermodynamic space. Hamada et al. pursue a more thermodynamic focus, employing model membranes containing DOPC, DPPC, and cholesterol at osmotically-induced elevated tensions [22]. They report an elevated demixing temperature at conditions expected to produce high tensions. (Here, tension favors phase separation.) They also find for the binary DOPC/DPPC system that, at conditions expected to elevate membrane tension, there is an elevation of the temperature for the first appearance of solid domains during cooling. In opposition to these findings, Portet and Keller employed

* Corresponding author. Tel.: +1 413 577 1417.
E-mail address: Santore@mail.pse.umass.edu (M.M. Santore).

http://dx.doi.org/10.1016/j.bbamem.2014.07.014
0005-2736/

micropipettes to quantitatively impose known tensions to mixed DOPC/DPPC/cholesterol vesicles [23]. They reported a tension-induced depression of the transition temperature.

We quantitatively probed the impact of tension, by micropipette aspiration of giant unilamellar vesicles and by separate osmotic manipulation, on the formation of DPPC-rich solid domains in mixed DOPC/DPPC membranes [24]. At a fixed composition of 30 mol% DOPC/70 mol% DPPC we found that membrane tension, during controlled cooling, depressed the temperature at which solid domains first appeared. These observations ran parallel to the report of Portet and Keller for the reduction of the liquid miscibility transition temperature [23]. In both cases elevated tension favored the less dense membrane phase, as would be expected based on fundamental arguments.

In single component lamellae, saturated phosphatidylcholines such as DPPC, DLPC, and DMPC form different solid-like bilayer phases because, when hydrated, differences in the sizes of their head and tail groups facilitate molecular tilt within the bilayer [25,26]. Solid bilayer phases include planar tilt ($L_{\beta'}$) also called a "gel", and a corrugated ($P_{\beta'}$) morphology, also called "rippled" [27–31]. In hydrated lamellar bulk samples, a first order melting peak (near 41.5 °C for DPPC [27]) marks the main transition from a pure fluid L_α phase to the $P_{\beta'}$ rippled solid. A second transition, termed the "pretransition," from the rippled solid phase to a tilted $L_{\beta'}$ solid phase occurs at a slightly lower temperature, in the case of DPPC near 35.5 °C [27]. In corrugated lamellae, the molecules are arranged almost perpendicular to the macroscopic membrane surface but at an angle from the local membrane tangent. The reported period of the corrugations for DPPC is ~16 nm though this can vary [32–34]. In the planar tilt phase the membrane is uniformly flat, and the molecules are at an angle of 29–32° from the membrane surface [35–37]. Notably, the angle of the molecules with the local surface normal is similar in the two configurations, making distinction of the two phases difficult by some methods. However, there is a clear exotherm on cooling from the corrugated to the tilt solid [26,38,39], and the areal density of the corrugated phase exceeds that of the tilt phase by ~10% [25]. (This areal density for the corrugated phase is based on the macroscopically apparent area, for instance the 2D projection normal to the large scale membrane direction.) This imparts a potential influence of tension on the phase transition.

In giant unilamellar vesicles of 30 mol% DOPC/70 mol% DPPC, we found evidence for two distinctly different types of solid domains, based on shape, dye uptake, and the temperatures at which they first appeared [24]. The occurrence of DPPC-rich striped and patchy domains in this system was previously reported [16,40–42] and dye selectivity was noted in careful studies by Feigenson [40,42]. Our assignment of the ripple phase to round or hexagonal DPPC domains and planar tilt to the DPPC-rich striped phase semi-quantitatively explained, using arguments from first principles, the tension sensitivity (imposed via micropipettes) of the transition temperature between these two solids in the giant unilamellar vesicles.

Extending our prior work at fixed composition, the current study examines the tension sensitivity of the phase separation and the nature of the domains for the DOPC/DPPC system over the full range of compositions, from temperatures near 25 °C up to the one phase region, and tensions from ~0 mN/m to that of lysis near 4 mN/m. Using both micropipette and osmotic manipulation of membrane tension, the 3D thermodynamic phase map is built and describes the coexistence of the L_α fluid, patchy solid, and striped solid DPPC domains. The assignment of the corrugated $P_{\beta'}$ structure to the patches and tilt $L_{\beta'}$ structure to the stripes is an interpretation that allows a simple fundamental model that qualitatively explains the shape of the phase diagram within the limits of the available physical property data. Reverse assignment of the two solid phases (patchy hexagons — tilt; stripes — corrugated) produces large qualitative discrepancies between the observations and a simple fundamental treatment.

2. Experimental description

2.1. Lipids

1,2-Dioleoyl-*sn*-glycero-3-phosphocholine and 1,2-dipalmitoyl-*sn*-glycero-3-phosphocholine (DOPC and DPPC respectively) were purchased from Avanti Polar Lipids (catalog numbers 850375C and 850355C) and used as provided. 1,2-Dioleoyl-*sn*-glycero-3-phosphoethanolamine-N-(lissamine rhodamine B sulfonyl) ammonium salt [Rh-DOPE, catalog number 810150C] and 1-2-dipalmitoyl-*sn*-glycero-3-phosphoethanolamine-N-(lissamine rhodamine B sulfonyl) ammonium salt, [Rh-DPPE, catalog number 810158C] were also purchased from Avanti and used as tracer lipids.

2.2. Vesicles

Vesicles were prepared by electroformation, a method established to produce substantial numbers of giant unilamellar vesicles [43]. DOPC and DPPC, in the desired molar proportions, were dissolved in chloroform near a concentration of 1 mg/ml. Rh-DPPE or Rh-DOPE tracers were employed at a concentration of 0.1 mol% relative to the total phospholipid. (Tracer concentrations of 0.1–0.5 mol% were found not to influence the phase separation temperatures.) A 10 μl quantity of phospholipid solution was placed on the platinum wire electrodes and, after drying under nitrogen, the chamber was sealed. It was then filled with DI (de-ionized) water or sucrose solution that had been preheated to 52 °C. An alternating current was applied to the electrodes at 3 V and 10 Hz for 1 h, while the chamber was maintained at 52 °C, to maintain the compositional uniformity of the vesicles. The vesicle solution was harvested in a syringe.

2.3. Micropipettes

Micropipette manipulation was employed to quantitatively control the tension of single vesicles during cooling and phase separation. Micropipettes, with inner tip diameters of 3–6 μm, were pulled on a Kopf Instruments Micropipette Puller. The tip shapes were refined using a Technical Products International Microforge so that the inner diameters were nearly constant in the region where vesicles projected into the pipettes. Bovine serum albumin (Sigma catalog number A7511) was adsorbed to the pipette tips to prevent vesicle adhesion. Vesicles were chosen in the 15–50 μm diameter range, at least 3 times greater than the pipette diameter, to avoid computational error in calculating tension and area. The tension of aspirated vesicles was controlled by applying suction using a siphon manometer. The uncertainty on the suction pressure was less than 1 mm head of water. Small errors (less than 10%) in measuring pipette and vesicle diameter, contributed to the overall uncertainty on tension of ~0.02 mN/m.

2.4. Phase separation

Vesicle phase separation was studied by fluorescence microscopy in two types of custom-built temperature-control chambers: open and closed. Both fit onto a Nikon Diaphot 300 inverted fluorescence microscope and controlled the rate of cooling. Images were obtained using a CoolSnap HQ CCD camera. Open sided chambers, made of coverslips supported in a gap configuration with a spacing of ~1 mm, allowed micropipette access from the side. The ends of the chamber were coupled to a temperature reservoir that was regulated by a heating bath. The open-sided chamber and the micropipettes themselves placed restrictions on experiments, necessitating additional studies with free vesicles in a closed chamber. First, micropipettes required long working distance objectives with less light gathering capability than is usual for fluorescence imaging. This compromised the image quality in micropipette studies compared to the closed chamber. Additionally, evaporation from the open chamber limited the experimental duration

to about 15 min. As a result, the slowest cooling rates, on the order of 0.1 °C/min, could be achieved only in the closed chamber.

Without micropipettes, phase separating vesicles in a closed chamber could be better imaged via higher numerical objectives. Without evaporation in the closed chamber, longer runs, a broader range of cooling rates in the range of 0.1–5 °C/min, and more precise temperature control was possible. Here a vesicle suspension was sealed in a ~125 μm gap between two coverslips.

In studies of phase separation and domain morphology, vesicles were transferred from the heated electroformer to one of the two test chambers where they were heated, placing them within the one-phase region, for at least 5 min. A cooling program was then initiated and phase separation and tension studies were then conducted. In these studies, vesicle tension was manipulated directly using micropipettes in the open chamber or, in the closed chamber, osmotic and other conditions were chosen to produce membrane tensions within a targeted range, as described below.

2.5. Osmotic pressure control of near-zero tension in the closed chamber

To produce flaccid vesicles with near-zero tensions over a range of temperatures, vesicles were osmotically conditioned. After electroformation in a 200 mOsm sucrose solution, vesicles were equilibrated in 250 mOsm sucrose solution. Over a few tens of minutes, water diffusion out of the vesicles made them flaccid. A measure of this "flaccidness" is the excess area, A_{xs}, defined relative to a sphere of the same volume

$$A_{xs} = \frac{A}{\left[36\pi V^2\right]^{\frac{1}{3}}} - 1. \quad (1)$$

Here A is the measured vesicle area and V is the measured vesicle volume, both determined from videomicrographs of vesicles aspirated into micropipettes at low suction (producing membrane tensions near 0.02 mN/m).

2.6. Vesicles with spontaneous elevated tensions in the closed chamber

In contrast to osmotically-conditioned flaccid vesicles, vesicles formed and equilibrated in DI water at elevated temperatures prior to cooling were observed not to exhibit excess area. These vesicles were instead found (as detailed below) to be tensed at room temperature following controlled cooling at rates of 1 °C/min. It is not obvious that this simple treatment produces elevated tensions. We discovered this to be the case and confirmed this with tension characterization studies, described next.

The hypothesized mechanism for the development of membrane stress was critical in the design of our characterization studies and is therefore described here: It involves a starting point at elevated temperatures, for instance near 50 °C in our studies, where vesicles exhibit little, if any, excess area, as we confirm below. Subsequent cooling causes both the vesicle membrane and its water contents to contract, as a natural consequence of their thermal expansivities [44]. The membrane, however, contracts more extensively than the aqueous vesicle center, causing development of membrane stress. The membrane stress relaxes as water diffuses out of the vesicles across the membrane, on a timescale of minutes [45–48]. Water transport across the membrane may be further increased by phase separation. Thus the actual values of the membrane stress and its variation with time depend on the cooling rate relative to that of water diffusion.

2.7. Characterizing stress of free vesicles, like those in the closed chamber

Characterization of the membrane stresses relevant to the phase transition(s) of vesicles cooling in the closed chamber required attention to the fact that, as a result of continued water diffusion from stressed vesicles, stresses measured at room temperature after vesicle phase separation would likely be lower than the stress occurring during phase separation itself. We therefore designed characterization studies that would probe the membrane tensions of vesicles cooled from 45 °C to a temperature of about 35 °C, in the range where phase separation had or was about to start. Further, because controlled cooling at different rates could not be accomplished reliably in the open chamber, vesicles were cooled at a programmed rate and then quickly transferred to a constant temperature micropipette (open) chamber for immediate characterization. Measurements were made within minutes, allowing some tension loss, but minimizing the loss as much as possible.

The stress state of vesicles was characterized by micropipettes by first attempting to aspirate at extremely low suctions, producing membrane stress in the range of 0.02–0.04 mN/m, corresponding to areal strains of less than 0.1%. For flaccid vesicles, a projection would appear in the micropipette and excess area could be quantified. Tensed vesicles, however, would be pulled to the mouth of the pipette but would not produce a projection. Subsequent increase in suction would produce a projection only once the suction pressure balanced the opposing force from the membrane tension. The suction pressure, P_s, corresponding to the first appearance of a projection allowed determination of the membrane tension, τ, of the stressed vesicles according to:

$$\tau = \frac{P_s R_p}{\left(2 - \frac{2R_p}{R_v}\right)}. \quad (2)$$

Here R_p and R_v are the micropipette and vesicle radius (outside the micropipette), respectively.

3. Results

3.1. Characterizing tension

While most of the phase diagram was mapped with tension manipulated quantitatively by micropipette aspiration during cooling, the best images of phase separated domains were obtained on free vesicles in the closed chamber. For the relevant cooling histories, Fig. 1 summarizes separate characterization studies of the membrane tension of free vesicles like those in the images in the next sections, below. Important to note, tension was measured at three different points (in separate studies) in the cooling history: 1. before cooling, 2. at conditions intended to approach those corresponding to the first instants of phase separation, and 3. later at room temperature.

Fig. 1 enforces several important points: (1) Vesicles conditioned in sucrose maintain near-zero tensions before, during cooling, and after cooling. (2) Vesicles cooled at 1 °C/min in DI water from 45 °C to about 35 °C experience substantially elevated tensions. (3) Vesicles cooled at 1 °C/min in DI water from 45 °C to room temperature and characterized within 15 min register a tension loss back to near zero tension. (4) With greater DPPC content in vesicles processed in DI water, it appears that slightly higher stresses are observed on cooling, and (5) faster cooling at 5 °C/min produces, for vesicles processed in DI water, lower tensions than cooling at 1 °C/min.

The first three points are consistent with the hypothesis that thermal contractions of the membrane, relative to those of the water, produce stress, which tends to relax with time, presumably by water diffusion across the membrane. Additionally, in point 4, the observation of increased tension at 35 °C with increased DPPC content may result from greater amounts of solid domains (demonstrated below) in these vesicles. With the solid domains being denser than the fluid domains, their formation causes extra areal reduction compared with the thermal contraction alone.

Finally for vesicles in DI water, the observation of lower finite stress with fast cooling at 5 °C/min is consistent with vesicle rupture and resealing (and continued thermal contraction) [49–51]. We find that

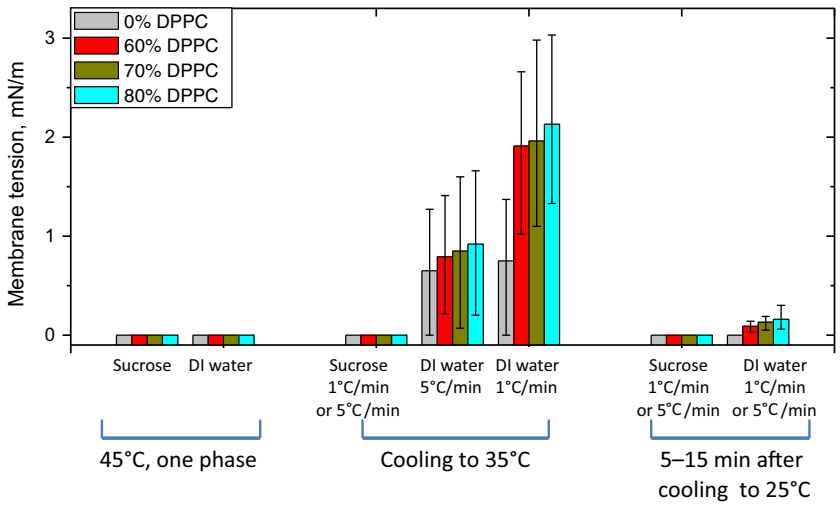

Fig. 1. Tensions measured for 10–15 vesicles at each condition, using micropipettes. Error bars represent the full range of observed tensions. (When vesicles were flaccid, all vesicles exhibited zero tension and so no error bars are shown.).

vesicles with 30% DOPC/70% DPPC exhibit a lysis strain of ~4% at room temperature. However, with a reported area-based thermal expansion coefficient of 4.2–6.8 × 10^{-3} K^{-1} in phosphatidylcholine membranes [44], cooling from 45 to 25 °C would produce an area reduction on the order of 10%. Depending on the original water content of the vesicle, with limited time for water diffusion of the central pool (for fast cooling), there is certainty of vesicle rupture. While we cannot see rupture happening because resealing is relatively rapid, Fig. 1 establishes the membrane tensions for these different histories, most of which are relevant to the images in Figs. 2–4. Only one history, cooling at 1 °C/min in DI water was employed to generate a limited portion of the phase map in Fig. 6. For the other data in the phase map, phase separation temperatures from measurements in the closed chamber were compared to micropipette studies with carefully controlled tensions.

3.2. Qualitative features

3.2.1. Appearance at room temperature

The fluorescence micrographs in Fig. 2 show the influence of the overall DOPC/DPPC ratio on the appearance of solid domains for a series of vesicles processed in DI water and cooled from the 1-phase region above 45 °C to room temperature where the images were recorded. These vesicles contain 0.1 mol% Rh-DOPE tracer which, by concentrating in the fluid L_α membrane phase, reveals the solid domains from which tracer is excluded. These images are typical of all vesicles in this size range within the imaging chamber (we did not scrutinize vesicles below 10 μm) and were reproduced for more than 5 electroforming batches each. In this series, tension depends on the cooling rate, and is elevated at 1 °C/min and low but non-zero at 5 °C/min, (see Fig. 1.)

With low but non-zero membrane tensions (achieved by cooling at 5 °C/min), vesicles exhibited patchy or irregular hexagonal-shaped dark domains if they contained 35 mol% DPPC or greater. Vesicles with lower DPPC content appeared uniform. Besides the exclusion of tracer, further evidence for the solid-like nature of the patchy dark domains includes their fixed shape and lack of coalescence. The increasing dark patch area with increased overall DPPC content argues that the patchy domains are DPPC-rich. These observations are consistent with the long literature on 2-component vesicles in which DPPC comprises the higher melting of the two phospholipid components. Phase separation on cooling produces solid domains composed predominantly of DPPC, suspended within the two-component fluid L_α phase [8,52,53]. Recent careful studies report a DPPC content in the solid between 90 and 95% though a distinction between gel and ripple phase is not made, or the gel is assumed [52,54].

In Fig. 2, vesicles experience higher tensions if cooled more slowly at 1 °C/min. The resulting dark domains appear as stripes instead of patches at room temperature and increase in area as the overall DPPC content is increased. This indicates that the stripes are DPPC-rich.

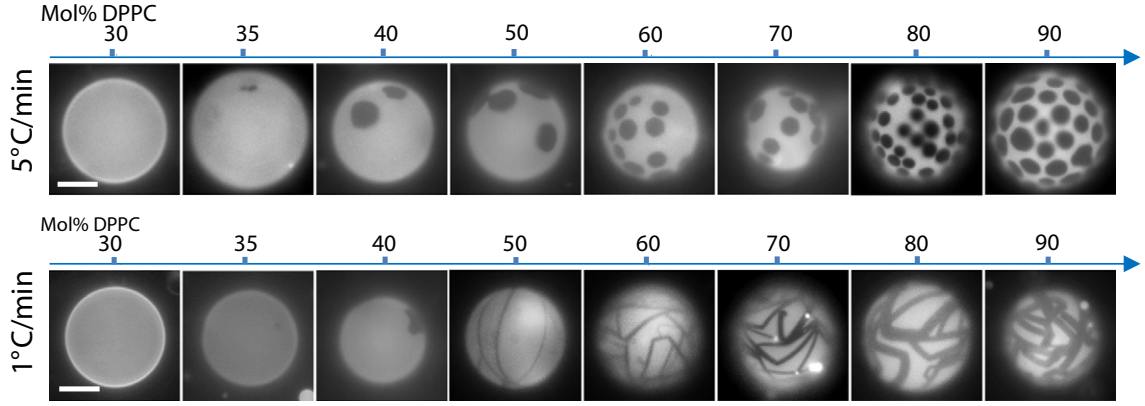

Fig. 2. Typical appearance of vesicles, for different DOPC/DPPC compositions, and using an Rh-DOPE tracer. The upper series is for cooling at 5 °C/min and the lower series is for cooling at 1 °C/min, both in DI water. The vesicles were imaged at 25 °C. The scale bar is 10 μm.

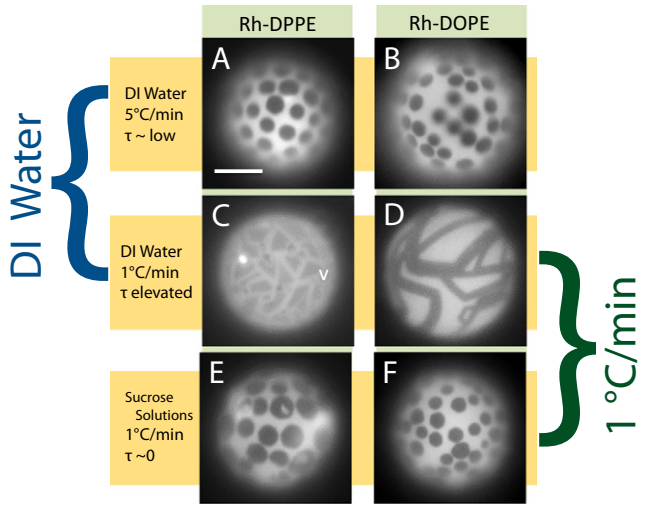

Fig. 3. Influence of processing parameters on the formation of patches or stripes, comparing the uptake or exclusion of 0.1 mol% tracer dyes: Rh-DPPE or Rh-DOPE. Labels in beige boxes indicate conditions for each vesicle. All have 20/80 mol ratio DOPC/DPPC. Scale bar is 10 μm.

Stripes are not seen when the overall vesicle composition is below ~50% DPPC.

Fig. 2 raises the question of whether the appearance of stripes versus patches is purely morphological or if there are deeper underlying thermodynamic differences in the solids, for instance in molecular arrangements. Figs. 3A–D address this question by comparing, at room temperature, the appearance of vesicles like those in Fig. 2 at a fixed composition (20/80 mol% DOPC/DPPC), but employing different tracer dyes. (Fig. 3A–D is like Fig. 2 in that they are cooled at 5 °C/min or 1 °C/min in DI water.) While patches exclude both Rh-DOPE and Rh-DPPE tracers, the stripes selectively include Rh-DPPE but exclude Rh-DOPE. This selectivity makes a compelling argument for different molecular arrangements and/or compositions (especially mol% DPPC) within the two types of solid domains.

From Fig. 2 and just the 4 images in Fig. 3A–D it is not clear which parameter, membrane stress or cooling rate fundamentally determines whether a vesicle will form striped or patchy solid domains. Figs. 3C–F, which show vesicles at a fixed cooling rate at 1 °C/min, isolate the impact of tension. In DI water, cooling at 1 °C/min produces elevated tensions and striped domains. Conversely, with tension osmotically fixed near 0 mN/m, the same cooling rate produces patch-shaped domains. In this range of cooling rates, therefore, the tension, not the cooling rate, determines the types of domains.

3.2.2. Cooling sequences

Fig. 4 shows sequential micrographs for a vesicle with 30/70 mol% DOPC/DPPC during cooling at low tension. The sequence in part A with rapid cooling at 5 °C/min shows that, on a single vesicle, similarly-sized small domains first appear and then grow with time. The apparent mechanism of nucleation and growth will be fully explored in a future paper. Important here is the persistence of the patchy domains at cool temperatures, due to kinetic trapping during rapid cooling.

The kinetic trapping that occurs on rapid cooling contrasts with the vesicle appearance and development of domains in slow cooling in Fig. 4B. Vesicles of the same 30/70 mol% DOPC/DPPC composition in Fig. 4B are osmotically conditioned in sucrose solutions to maintain a near zero tension during an extremely slow cooling rate of 0.1 °C/min. Fig. 4B demonstrates the initial appearance of patches, followed by their growth and their subsequent complete conversion to stripes with progressive cooling.

A comparison of Figs. 4A and B reveals that the cooling rate has a minimal influence on the temperature corresponding to the first appearance of patches (38.3 ± 0.5 °C here). While we expect some influence of kinetics determining when domains are first visible, this effect here is less than 1 °C. b) The cooling rate can, however, dictate whether patches or stripes are ultimately seen at room temperature. We believe that the complete conversion of patches to stripes at low temperatures and very slow cooling indicates that stripes are the preferred (stable equilibrium) phase at lower temperatures. The persistence of large patches after rapid cooling to low temperatures may indicate a kinetic trapping of a robust metastable equilibrium: Conversion of large solid domains from one molecular arrangement to another would involve a large energy barrier and was not observed at room temperature on a timescale of tens of minutes.

Additionally, with regard to Fig. 4B we observed, with repeat runs with different vesicles, that the temperature for the first appearance of stripes (in the presence of patches) is distinct and is a function of composition (as we will show). The conversion of patches to stripes occurs in less than 5 min at the cooling rate of 0.1 °C/min, and therefore the two types of solid domains coexist only over a narrow temperature range (less than 0.5 °C). Whether this represents a true equilibrium envelope or a single solid–solid transition point at a fixed temperature for each composition is unclear. Additionally regarding the striped domains, no ends are visible: They intersect each other or they intersect patches. Even when they are first visible the stripes are already long and an increase in length is not visible. More and wider stripes develop with further cooling once the patches are consumed.

3.2.3. Qualitative features of phase separation micropipettes

While we can osmotically manipulate vesicles to produce an excess area and thereby maintain a near zero tension during cooling, it is not possible to maintain a fixed known elevated tension during cooling

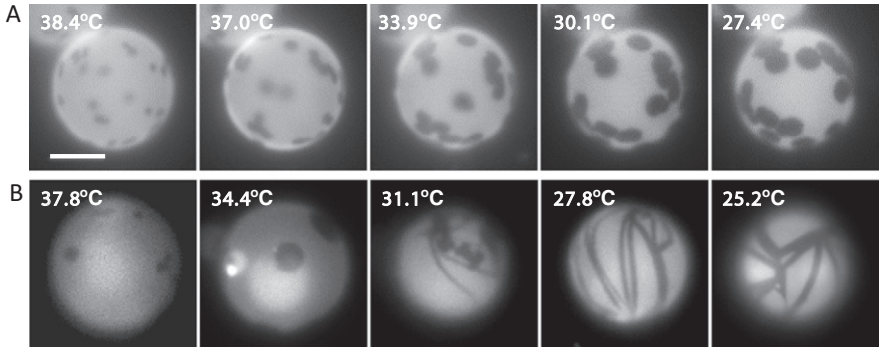

Fig. 4. Domain growth during cooling in DI water for vesicles with a composition of 30/70 mol ratio DOPC/DPPC. (A) Cooling at 5 ° C/min, from Ref. [24]. Here the tension is relatively low. (B) A series of vesicles during very slow cooling at 0.1 °C/min in sucrose to maintain tension near zero.

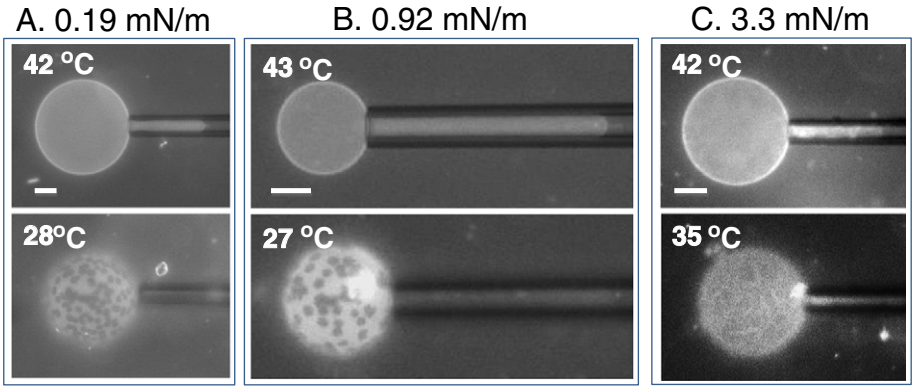

Fig. 5. Images of vesicles in micropipettes before and after phase separation at the temperatures and tensions indicated. Tension is fixed throughout the cooling process. The molar ratio of DOPC/DPPC is 20/80 and 0.1 mol% Rh-DPPE tracer dye has been added. Each scale bar is 10 μm.

by osmotic conditioning. To achieve quantitative control of elevated membrane tensions, we employed micropipettes, but at the sacrifice of image quality and ability to achieve slow cooling. As an example of micropipette manipulation, the images in Fig. 5 illustrate, for three different fixed tensions, the appearance of solid phases during the cooling process. While micropipettes quantify membrane tension, facilitating construction of phase maps below, important qualitative features are highlighted here: At higher tensions, above 3 mN/m for the composition in Fig. 5, a striped solid phase was seen to form directly from the fluid. In micropipettes, patches are not usually seen to convert to stripes because cooling is usually sufficiently rapid to kinetically trap the patchy solid domains, consistent with Fig. 4.

3.2.4. Summary of qualitative findings

Even without precise quantification of tension or temperature it is evident that domains of thermodynamically different solids can be observed, depending on vesicle composition and tension and, to a lesser extent in certain cases, cooling history. Striped domains are seen in two situations: 1) they form, at the highest fixed tensions, directly from the one-phase fluid during moderate cooling (1–2 °C/min, no other cooling rates could be tested) in micropipettes and 2) at lower tensions and with sufficiently slow cooling (0.1 °C/min), stripes can be produced by the conversion of previously formed hexagonal patchy domains. The striped domains observed in DI water in Fig. 2, with the elevated membrane tension, could fit into either of these categories depending on the vesicle tension at the instant of phase separation, as discussed below. Patchy hexagonal domains, on the other hand, form directly from the one phase fluid mixture at low and moderate tensions, fairly independent of cooling rate. However, with time and especially for slow cooling they tend to convert to stripes. The patches are stabilized however, by rapid cooling that produces large domains. The patchy domains are distinctly different in their molecular arrangement from the stripes, evidenced by selective incorporation of tracer dyes. Patchy solid domains have never been observed at substantially elevated tensions, for instance 3 mN/m.

These observations suggest that tension is a fundamentally important thermodynamic variable influencing more than domain size and therefore visibility. The next section further explores the phase diagram of DOPC/DPPC in temperature–tension–composition space.

3.3. Phase maps

Fig. 6 shows different representations of the three dimensional phase map of the DOPC/DPPC mixture, measured by noting the temperature and shape of the first appearance of solid domains when vesicles were cooled from the one phase region. Here temperature, composition, and tension are the three independent variables defining a 3-dimensional thermodynamic space in Fig. 6A. While it is difficult to see the details, there are three "branches" or curved planes intersecting in this three dimensional space. (The tiny section on the high-tension side of the dashed line is a separate branch easily overlooked.) These represent fluid–patch solid coexistence, fluid–stripe coexistence, and patch–stripe coexistence. Because of the complexity of the experimental results in Fig. 6A, we additionally present slices through this space, at constant composition (Fig. 6B) or constant tension (Fig. 6C). The particular features of the phase diagram are discussed in the context of these constant composition and tension sections, which are easier to see.

With a few exceptions noted below, micropipettes were employed to control tension and elucidate the solid DPPC-rich domain formation, typically patches at low tension and stripes at high tension (hollow points). Probing the tension dependence of the patch-to-stripe transition required our best imaging and slow cooling, neither possible in micropipettes. Therefore, the patch to stripe transition was tracked in the closed chamber (solid points).

Fig. 6B presents temperature–composition plots at a series of fixed tensions. Fig. 6Bi shows, for clarity, data collected exclusively at zero tension. Then in Fig. 6Bii additional curves for data at elevated tensions are included. At zero tension in Fig. 6Bi the upper data set shows the temperatures at which solid DPPC-rich domains were first observed on cooling. All of these initially-formed solid domains turned out to be patch-shaped. The data approach the reported melting transition of pure DPPC (41.5 °C [27]) as the proportion of DPPC is increased in the mixture. As the DPPC is increasingly diluted with DOPC, the appearance of patch-shaped DPPC-rich domains occurs at progressively lower temperatures, as expected for the classical case of melting point depression.

The lower curve in Fig. 6Bi summarizes the temperatures for the patch-to stripe transition measured with the same vesicles, still at $\tau \sim 0$, employed to determine the upper curve. It is interesting that this lower curve extrapolates, in the limit of high DPPC concentrations, to the so-called "pretransition" reported for the conversion between a ripple solid and tilted solid phase in pure DPPC (35.5 °C [27]). The significance of this will be discussed in the following section.

Fig. 6Bii expands the content Fig. 6Bi with additional temperature–composition curves (solid lines) measured in micropipettes, each at a different fixed tension. Each curve constitutes a different slice through the 3-dimensional map of Fig. 6A. On each of these fixed-tension solid curves, patch-shaped DPPC-rich solid domains first appear from the cooling fluid membrane and the temperature of their first appearance shifts downward slightly with increases in tension. It is gratifying that the temperatures measured near zero tension (0.02 mN/m) in micropipettes for patch appearance agree well with the temperatures recorded for vesicles osmotically conditioned with sucrose to near zero tension in the closed chamber. At tensions exceeding ~3 mN/m, the first solid DPPC-rich domains to form from the fluid were stripes, not patches. The points for the

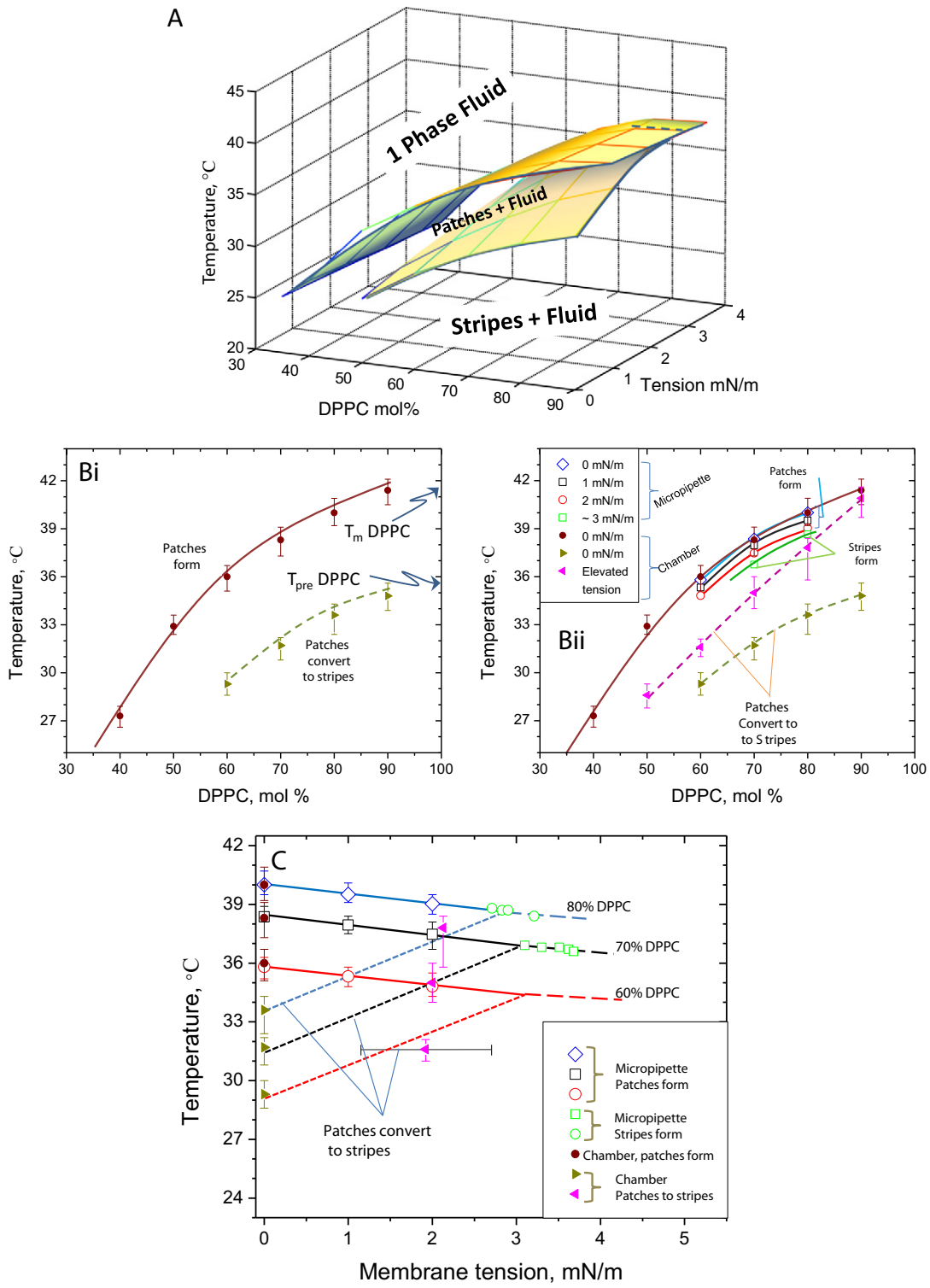

Fig. 6. A. Three dimensional phase space of DOPC/DPPC membranes (temperature, tension, total DPPC content) from an angle that looks into the region where patches (ripple phase) form. From other angles the region containing patch-fluid equilibrium pinches closed. Bi. Temperatures for the first appearance of patches and for their conversion to stripes in zero-tension vesicles. Near-zero tension was maintained by osmotically conditioning in sucrose solutions. Bii. Controlled-tension sections through DOPC–DPPC phase space, indicating the first appearance of patches or stripes as a function of temperature, with solid curves guiding the eye. The conversion of patches to stripes is indicated with dashed lines. Hollow data points are obtained in micropipettes with tensions as indicated. Solid points were obtained in the closed chamber. Here the zero tension data is precisely controlled through choice of sucrose solutions, while the elevated tension data carries a large uncertainty for cooling in DI water at 1 °C/min as indicated in Fig. 1. C. Temperature-tension sections of DOPC/DPPC phase space, with slices for different overall compositions. Error bar on lower pink triangle datum is typical only of all the pink triangle data (for conversion of patches to stripes in chamber in DI water). The uncertainty on tension for the other data is 0.02 mN/m. The lines are calculated based on the model discussed below.

appearance of striped DPPC-rich domains directly from the fluid on cooling in micropipettes are also included but will be shown to fall on a separate branch of the phase diagram.

In addition to the zero-tension dashed curve for the conversion of patches to stripes (from Fig. 6Bi) Fig. 6Bii also includes a data set (also a dashed line) at elevated tensions for the conversion of patches

to stripes. Here the elevated tension was achieved in the closed chamber in DI water by cooling at 1 °C/min, and thus carries a large uncertainty. Additionally, for this data set, the tension at the moment of phase separation varies slightly (consistent with Fig. 1) with composition. Nonetheless, it is clear that the patch–stripe conversion temperature increases with imposed membrane tension.

It is worth emphasizing that, while temperature–composition maps for DPPC mixed with other phospholipids have been reported many times previously [8,55,56], the data in Fig. 6B differ in their quantification of tension and its assurance of a constant value for each curve (excepting the pink dashes where tension varies as described in Fig. 1.)

Fig. 6C, which presents temperature–tension curves at different fixed overall compositions, explicitly shows the impact of tension on the observed transitions. These data are the same as those in Fig. 6A and Bii, now on different axes. The lines represent a model, described below.

In the temperature–tension perspective of Fig. 6C, the three-branch nature of the thermodynamic space is evident. The upper branch at tensions less than ~3 mN/m describes the first appearance, with progressive cooling, of patch-shaped DPPC-rich solid domains in the fluid membrane. At tensions exceeding ~3 mN/m (depending on composition) the striped-shaped DPPC-rich solid domains are the first and only phase to appear on cooling, constituting a separate branch. Finally at low tensions and temperatures a third branch describes the transition of patchy to striped domains in the presence of the fluid membrane. Importantly, the upper two branches, for the first appearance of solid or striped domains in the fluid, both have slightly negative slopes. The lower branch for the patch to striped transition has a positive slope and intersects the upper branches creating a triple-point-like feature at each composition.

A few points are worth making. First near zero tension (on the left axis) temperatures measured for the first appearance of patch-shaped domains in the closed chamber (at the ultraslow cooling rate) show excellent agreement with those measured in micropipettes and cooled at a rate of 1–2 °C/min. Further, at zero tension, the data for the conversion of patches to stripes are obtained by osmotically conditioning vesicles with sucrose solutions and cooling at 0.1 °C/min. The patch to stripe transition was inconsistently seen in micropipettes because micropipettes necessitate a faster cooling rate, which tends to kinetically trap large patchy domains, demonstrated in Fig. 4.

For clarification, we mention that all the data on the upper two branches of Fig. 6C were measured using micropipettes for tension control, except at zero tension where data points from both micropipettes and osmotic manipulation agree well. Below tensions of about 3 mN/m, data points are averages based on 10 vesicles. At tensions above 3 mN/m, rupture limited the numbers of vesicles that could be studied so data are plotted for individual vesicles.

Finally worth highlighting are data for the patch-to-stripe transition at elevated tensions near 2 mN/m, the pink triangles in Fig. 6C. (These are the same pink triangles on the pink dashed line in Fig. 6Bii.) These data are the only stand-alone data on the phase diagram obtained in the closed chamber. The points each represent an average of temperatures measured at the patch-to stripe transition temperatures for 10–15 vesicles at each composition. The data carries a large uncertainty in tension, but they fit well on each of the three calculated lines (model to be presented below), suggesting a stronger tension-sensitivity of the patch to stripe transition than the other two branches.

A key feature of the phase diagram is the triple point-like feature that is most evident in Fig. 6C for each composition when transition temperature was mapped as a function of tension. The triple points are not clear in the familiar temperature–composition representation (Fig. 6B) but, in the 3D space of Fig. 6A, they appear as a line (a locus of triple points) where the three curved surfaces intersect. The "triple point locus" marks, for a particular composition, the tension above which patch-shaped domains are not seen. As a result, for tensions above the triple point locus, cooling vesicles into the one phase region always produces striped domains irrespective of the cooling rate. In this way, tension regulates the choice of solid formed and the related domain morphology, somewhat independent of cooling rate.

3.4. A model for the effect of tension on the transition temperature

A simple first-principles treatment provides an interpretation of the phase diagram and, in particular the shapes of the temperature–tension curves in Fig. 6C. The treatment starts with the general fundamental expression for chemical equilibrium expressed in differential form as found in textbooks [57]. Treating the negative membrane tension as the two dimensional (2-D) analog of pressure, and considering area rather than volume, a 2-D membrane version of the general expression results, written here for a fluid–solid transition of a binary mixture:

$$\left(\frac{\partial\tau}{\partial T}\right)_{x^{\mathrm{liq}}_{\mathrm{DPPC}},(\mathrm{solid-liq})} = -\frac{1}{T}\frac{x^{\mathrm{solid}}_{\mathrm{DPPC}}\left(\overline{H}^{\mathrm{solid}}_{\mathrm{DPPC}}-\overline{H}^{\mathrm{liq}}_{\mathrm{DPPC}}\right)+x^{\mathrm{solid}}_{\mathrm{DOPC}}\left(\overline{H}^{\mathrm{solid}}_{\mathrm{DOPC}}-\overline{H}^{\mathrm{liq}}_{\mathrm{DOPC}}\right)}{x^{\mathrm{solid}}_{\mathrm{DPPC}}\left(\overline{A}^{\mathrm{solid}}_{\mathrm{DPPC}}-\overline{A}^{\mathrm{liq}}_{\mathrm{DPPC}}\right)+x^{\mathrm{solid}}_{\mathrm{DOPC}}\left(\overline{A}^{\mathrm{solid}}_{\mathrm{DOPC}}-\overline{A}^{\mathrm{liq}}_{\mathrm{DOPC}}\right)}. \quad (3)$$

This expression relates temperature and tension along the 2-phase coexistence curve at constant composition ($x^{\mathrm{liq}}_{\mathrm{DPPC}}$). It can be applied separately to the equilibrium between the patchy solid and the fluid or between the striped solid and the fluid. x^{α}_{a} refers to the mole fraction of component a (DOPC or DPPC) in phase α (solid or liquid). H denotes enthalpy and A denotes area, and the overbars refer to partial molar properties. At this point, either phase can contain both components in any proportion. A version of the expression for equilibrium between the patchy solid and striped solid would look the same, substituting a second solid superscript for the liquid superscript.

Simplifying assumptions were made only at this point: The fluid L_α phase was treated as an ideal solution while either solid phase was treated as being pure DPPC. (Now the partial molar properties become equal to the pure solution properties on a molar basis. Additionally $x^{\mathrm{solid}}_{\mathrm{DPPC}}=1$ while $x^{\mathrm{solid}}_{\mathrm{DOPC}}=0$) This led to:

$$\left(\frac{\partial T}{\partial \tau}\right)_{x^{\mathrm{liq}}_{\mathrm{DPPC}},(\mathrm{solid-liq})} = -T\frac{\Delta A^{\mathrm{solid-liq}}_{\mathrm{DPPC}}}{\Delta H^{\mathrm{solid-liq}}_{\mathrm{DPPC}}}. \quad (4)$$

In Eq. (4), the slope of the coexistence curve depends only on the temperature and the area and enthalpy changes at the transition.

The simplifications of a pure solid and an ideal solution are practical because of the absence of physical property data on partial molar areas and enthalpies, but they also turn out to be good estimates from the physical perspective. Over the temperature range of interest, the binary DOPC/DPPC fluid is reasonably approximated by an ideal solution: The temperature–composition curves of Fig. 6Bi, at zero tension, are of the general shape described by ideal solution behavior. Additionally consistent with ideal solution behavior, very similar curves for the first appearance of solid at low tensions are found for DPPC mixed with DLPC (1,2-dilauroyl-*sn*-glycero-3-phosphocholine) [56] or POPC (1-palmitoyl-2-oleoyl-*sn*-glycero-3-phosphocholine) [55]. The choice of second component does not matter for an ideal solution. Second, a moderate amount of a second species (up to 30% for instance, as an extreme test of the model) in the solid phase, turns out not to change the calculated slopes by more than a factor of two, even if relatively extreme physical property data values are arbitrarily substituted for the partial molar properties of the DOPC [24].

From Eq. (4), the slopes of lines estimating the tension sensitivity of phase transition temperatures were calculated. Table 1 summarizes the calculations, using physical property data from the literature. Important in making this calculation, the physical properties of the corrugated DPPC phase are assigned to the patches and the planar tilt phase to the stripes. Lines having the calculated slopes were drawn in

Table 1
Calculated slopes of coexistence curves in temperature–tension space[a].

	$\Delta H^{\alpha-\beta}_{DPPC}$, cal/gDPPC	$\Delta A^{\alpha-\beta}_{DPPC}$, Å^2/DPPC	$\left(\frac{\partial T}{\partial \tau}\right)_{x^{\beta}_{DPPC},(\alpha-\beta)}$, K/(mN/m)
Ripple solid–fluid, 38 °C	−11.5	−10.7	−0.56
Tilt solid–ripple solid, 31.6 °C	−1.5	4.4	1.75
Tilt solid–fluid, ~37 °C	−13	−6.3	−0.29

[a] Transition temperatures are based on observations near zero tension for 70% DPPC.

Fig. 6C, starting with the phase transition temperatures measured at low tension.

The calculation reasonably approximates the data in Fig. 6C, but is not expected to be fully quantitative. Worth noting, the composition dependence of $dT/d\tau$ vanishes in Eq. (4), so nearly the same slopes are calculated for the transition lines at the different compositions in Fig. 6C. Because composition influences the transition temperature (per Fig. 6B), and because $dT/d\tau$ is proportional to the temperature in Eq. (4), there turns out to be a very slight effect (less than 1% in the range of interest) of composition on the calculated slopes. Also, without physical property data at different elevated tensions, the zero tension physical property data are applied over the full range of Fig. 6C. In reality, some influence of tension on the physical properties would impart real curvature to the lines which have been drawn as straight. This would shift the positions of the "triple points" in ways difficult to anticipate. The presence of the triple points would, however, be preserved as long as the areal densities of the different phases retain the ranking that occurs at low tensions, which is almost sure to be the case.

We wish to emphasize a single important point by comparing the data and the calculation: Assigning the patch-shaped DPPC-rich phase as the ripple $P_{\beta'}$ phase and the striped DPPC-rich domains as the tilt $L_{\beta'}$ phase is necessary for qualitative agreement. Both solids are denser than the fluid L_α phase. As a result the membrane contracts upon cooling through the transition from the fluid to either solid. This imparts negative slopes, in Fig. 6C, to the two upper branches at low and high tensions respectively. The corrugated solid DPPC phase is, however, more dense than tilt phase and thus, upon cooling from the patch to the striped phase, the membrane expands. This produces a positive slope for the impact of tension on the patch-to-stripe transition. The positive slope on the lower branch is also responsible for the appearance of the "triple point" like feature for a fixed composition. Different assignments of the patches and stripes would have given slopes of the wrong sign and the triple point like feature would not occur. While the model is extremely basic, it captures the key experimental observations because of the correct assignment of the phases and because a ball park estimation of the physical property data is "good enough."

While others report different signs on $dT/d\tau$ [21,22], our first principles treatment argues that our phase diagrams in Fig. 6 are correct. Worth mentioning, our observed trend that tension favors the less dense phase agrees with the report of Portet in a different system [23]. Our work and Portet's quantify tension with micropipettes in contrast to the dissenting investigations where tension is manipulated osmotically. Those dissenting reports did not quantitatively confirm the membrane tensions.

4. Discussion: interpretation in terms of equilibrium

Overall we believe the phase diagram in Fig. 6 to be a reasonable approximation (within limits of measuring boundaries by the visual appearance of dark domains) of the equilibrium phase boundaries: With tension controlled, there were minimal effects of cooling rate on the temperature of first appearance of solid phase, patches or stripes from the L_α fluid. Studies at zero tension but with different cooling rates confirmed the (usually minor) influence of cooling rate. The only instance where we found rate to be important was in the patch-to-stripe transition. Here rapid cooling rates favored retention of the originally formed solid patchy domains: Stabilization of DPPC-rich patch-shaped domains by rapid cooling into a region of the phase diagram where stripe-shaped domains were preferred likely produced large energy barriers to the conversion of the less-preferred patches to the more preferred stripes. However, even when the preferred stripe phase was kinetically disallowed, the proportions of patches (greater areal coverage with increased overall DPPC content) were consistent with equilibrium and a mass balance ("the inverse lever-arm rule"). This suggests that the DPPC-rich patch-shaped domains formed and trapped during rapid cooling represent a metastable or restricted equilibrium, rather than, for instance a glass. It further suggests that the boundaries for the first appearance of DPPC-rich patchy or striped-shaped domains from the one-phase fluid represent, over the full range of compositions, the equilibrium surface. The same curve for the first appearance of patches, for instance, is the locus of the ends of tie lines.

5. Conclusions

This study reports the complex three dimensional phase map for mixed DOPC/DPPC membranes and it relates the different solid domains observed in different regions of thermodynamic space to previously reported molecular packings. While the composition dependence of the fluid–solid phase separation temperature follows expectations from previous reports, the tension-dimension of the phase diagram is rich because of the presence of two distinctly different solid phases in different regions. Ultimately three different coexistence branches (curved planes) were discovered: One for the equilibrium of the ripple $P_{\beta'}$ (at low tension) solid with the L_α fluid, one for the equilibrium of the tilt gel $L_{\beta'}$ solid (at high tension) with the L_α fluid, and a third for the coexistence of the two solids in the presence of the L_α fluid. While the L_α fluid persists at high temperatures over a full range of tensions, the $L_{\beta'}$ solid is preferred at cool (room) temperatures over a wide range of tensions. At intermediate temperatures, on the order of 30–38 °C, the choice of solid is tension-sensitive: the ripple $P_{\beta'}$ phase occurs at low tensions and the $L_{\beta'}$ phase at higher tensions. The ripple $P_{\beta'}$ phase was found to always produce irregular patchy or hexagonal domains that excluded the tracer dyes considered, while the $L_{\beta'}$ solid appeared as stripes which could selectively incorporate some tracers.

Acknowledgements

This work was supported by the UMass MRSEC on Polymer Science NSF-0820506.

References

[1] D.A. Brown, E. London, Annu. Rev. Cell Dev. Biol. 14 (1998) 111.
[2] K. Simons, E. Ikonen, Nature 387 (1997) 569.
[3] T. Baumgart, S.T. Hess, W.W. Webb, Nature 425 (2003) 821.
[4] R. Lipowsky, R. Dimova, J. Phys. Condens. Matter 15 (2003) S31.
[5] H.T. McMahon, J.L. Gallop, Nature 438 (2005) 590.
[6] B.J. Peter, H.M. Kent, I.G. Mills, Y. Vallis, P.J.G. Butler, P.R. Evans, H.T. McMahon, Science 303 (2004) 495.
[7] M. Laradji, P.B.S. Kumar, J. Chem. Phys. (2005) 123.
[8] S.L. Veatch, S.L. Keller, Phys. Rev. Lett. 94 (2005) 148101.
[9] G.W. Feigenson, Annual Review of Biophysics and Biomolecular Structure, vol. 36, Annual Reviews, Palo Alto, 2007, p. 63.
[10] A.C. Brown, K.B. Towles, S.P. Wrenn, Langmuir 23 (2007) 11188.
[11] R.F.M. de Almeida, A. Fedorov, M. Prieto, Biophys. J. 85 (2003) 2406.
[12] R.S. Petruzielo, F.A. Heberle, P. Drazba, J. Katsaras, G.W. Feigenson, Biochim. Biophys. Acta Biomembr. 1828 (2013) 1302.
[13] A.K. Smith, J.H. Freed, J. Phys. Chem. B 113 (2009) 3957.
[14] S.L. Veatch, S.L. Keller, Biochim. Biophys. Acta Mol. Cell Res. 1746 (2005) 172.
[15] L.A. Bagatolli, E. Gratton, Biophys. J. 79 (2000) 434.
[16] V.D. Gordon, P.A. Beales, Z. Zhao, C. Blake, F.C. MacKintosh, P.D. Olmsted, M.E. Cates, S.U. Egelhaaf, W.C.K. Poon, J. Phys. Condens. Matter 18 (2006) L415.
[17] C.H. Huang, S.S. Li, Biochim. Biophys. Acta Rev. Biomembr. 1422 (1999) 273.

[18] M.B. Sankaram, D. Marsh, T.E. Thompson, Biophys. J. 63 (1992) 340.
[19] V. Schram, H.N. Lin, T.E. Thompson, Biophys. J. 71 (1996) 1811.
[20] J.L. Thewalt, M. Bloom, Biophys. J. 63 (1992) 1176.
[21] A.G. Ayuyan, F.S. Cohen, Biophys. J. 94 (2008) 2654.
[22] T. Hamada, Y. Kishimoto, T. Nagasaki, M. Takagi, Soft Matter 7 (2011) 9061.
[23] T. Portet, S.E. Gordon, S.L. Keller, Biophys. J. 103 (2012) L35.
[24] D. Chen, M.M. Santore, Proc. Natl. Acad. Sci. U. S. A. 111 (2014) 179.
[25] D. Needham, E. Evans, Biochemistry 27 (1988) 8261.
[26] R. Lewis, N. Mak, R.N. McElhaney, Biochemistry 26 (1987) 6118.
[27] S. Tristram-Nagle, J.F. Nagle, Chem. Phys. Lipids 127 (2004) 3.
[28] D. Pentak, W.W.S. Kowski, A. Sulkowska, J. Therm. Anal. Calorim. 93 (2008) 471.
[29] K. Sengupta, V.A. Raghunathan, J. Katsaras, Phys. Rev. E. 68 (2003) 031710.
[30] M.J. Janiak, D.M. Small, G.G. Shipley, J. Biol. Chem. 254 (1979) 6068.
[31] Ph. Ververga, Hj Vandenbe, A.J. Luitingh, P.F. Elbers, Cytobiologie 6 (1972) 86.
[32] J. Katsaras, S. Tristram-Nagle, Y. Liu, R.L. Headrick, E. Fontes, P.C. Mason, J.F. Nagle, Phys. Rev. E. 61 (2000) 5668.
[33] J.A.N. Zasadzinski, Biochim. Biophys. Acta 946 (1988) 235.
[34] R. Vladkova, K. Teuchner, D. Leupold, R. Koynova, B. Tenchov, Biophys. Chem. 84 (2000) 159.
[35] A. Erbe, R. Sigel, Eur. Phys. J. E 22 (2007) 303.
[36] S. Tristram-Nagle, R. Zhang, R.M. Suter, C.R. Worthington, W.J. Sun, J.F. Nagle, Biophys. J. 64 (1993) 1097.
[37] P.N. Yi, Rc Macdonal, Chem. Phys. Lipids 11 (1973) 114.
[38] B.G. Tenchov, H. Yao, I. Hatta, Biophys. J. 56 (1989) 757.
[39] C. Grabielle-Madelmont, R. Perron, J. Colloid Interface Sci. 95 (1983) 471.
[40] G.W. Feigenson, J.T. Buboltz, Biophys. J. 80 (2001) 2775.
[41] L. Li, J.X. Cheng, Biochemistry 45 (2006) 11819.
[42] J. Korlach, P. Schwille, W.W. Webb, G.W. Feigenson, Proc. Natl. Acad. Sci. U. S. A. 96 (1999) 8461.
[43] M.I. Angelova, D.S. Dimitrov, Faraday Discuss. 81 (1986) 303.
[44] E. Evans, D. Needham, J. Phys. Chem. 91 (1987) 4219.
[45] D. Huster, A.J. Jin, K. Arnold, K. Gawrisch, Biophys. J. 73 (1997) 855.
[46] J.P. Spineni, R. Grosescu, M. Lupu, V. Dobre, Rev. Roum. Biochim. 20 (1983) 271.
[47] M. Bloom, E. Evans, O.G. Mouritsen, Q. Rev. Biophys. 24 (1991) 293.
[48] Needham, D., Zhelev, D. *Chapter 9*; Dekker: New York, 1996.
[49] D. Massenburg, B.R. Lentz, Biochemistry 32 (1993) 9172.
[50] K.A. Riske, R. Dimova, Biophys. J. 88 (2005) 1143.
[51] K.A. Riske, R.L. Knorr, R. Dimova, Soft Matter 5 (2009) 1983.
[52] M.L. Schmidt, L. Ziani, M. Boudreau, J.H. Davis, J. Chem. Phys. 131 (2009) 175103.
[53] R. Elliott, K. Katsov, M. Schick, I. Szleifer, J. Chem. Phys. 122 (2005) 044904.
[54] J. Juhasz, F.J. Sharom, J.H. Davis, Biochim. Biophys. Acta Biomembr. 1788 (2009) 2541.
[55] S.D. Shoemaker, T.K. Vanderlick, Biophys. J. 84 (2003) 998.
[56] F.A. Heberle, J.T. Buboltz, D. Stringer, G.W. Feigenson, Biochim. Biophys. Acta Mol. Cell Res. 1746 (2005) 186.
[57] M. Modell, R.C. Reid, Thermodynamics and Its Applications, 2 ed. Prentice Hall, Englewood Cliffs, NJ, 1983. (Vol. eqn 10–22).